

# Intraband and interband processes in the infrared spectrum of metallic aluminum

D. Y. Smith\*

*Materials Science and Technology Division, Argonne National Laboratory, Argonne, Illinois 60439*

B. Segall

*Case Western Reserve University, Cleveland, Ohio 44106 and Materials Science and Technology Division, Argonne National Laboratory, Argonne, Illinois 60439*

(Received 12 December 1985)

The dielectric function of polycrystalline metallic aluminum derived by Shiles *et al.* [Phys. Rev. B **22**, 1612 (1980)] from room-temperature ultrahigh-vacuum reflectance measurements has been analyzed into intraband and interband components and compared with theoretical predictions of Szmulowicz and Segall [Phys. Rev. B **24**, 892 (1981)]. For this analysis, a new approach was developed, which utilizes experimental data over a larger energy range than in previous studies. To within experimental uncertainty, the resulting intraband component is consistent with a Drude model having a plasma frequency  $\Omega_p = 12.5 \pm 0.3$  eV and relaxation time  $\tau = (1.06 \pm 0.12) \times 10^{-14}$  sec. These values are in accord with the bulk static conductivity which in turn is in agreement with the inertial sum rule on the real part of the dielectric function. The interband contribution was found to consist of a broad background with two superimposed peaks: the well-known "0.8  $\mu\text{m}$ " absorption at  $\sim 1.5$  eV and a weaker absorption in the vicinity of 0.4 eV. This interband spectrum is in good agreement in regard to both peak position and oscillator strength with the one-electron augmented-plane-wave model calculations for the optical conductivity by Szmulowicz and Segall. The total experimental intraband and interband oscillator strengths for the conduction electrons are 1.9 and 1.2 electrons/per atom, respectively.

## I. INTRODUCTION

In this paper we relate the results of two recent publications<sup>1,2</sup> on the optical properties of metallic aluminum. We show that the measured room-temperature optical conductivity<sup>1</sup> above  $\sim 0.1$  eV is in good agreement with predictions of augmented-plane-wave (APW) band-structure calculations,<sup>2</sup> on the conventional assumption that the observed dielectric function is the sum of an interband response and a Drude-model intraband contribution with frequency-independent parameters.

Shiles *et al.*<sup>1</sup> have recently reported a self-consistent Kramers-Kronig analysis of room-temperature optical and electron-energy-loss spectra for polycrystalline aluminum over the energy range of 0.04 to 10 000 eV. Their results satisfy all the major optical sum rules,<sup>3,4</sup> are in agreement with stopping-power measurements,<sup>5</sup> and are believed to be as free as possible of assumptions associated with specific models for the optical response. Below  $\sim 11.8$  eV, this analysis was based primarily on reflectance measurements for evaporated films prepared in ultrahigh vacuum as reported by Bennett *et al.*<sup>6</sup> and by Endriz and Spicer,<sup>7</sup> see Fig. 1. These data are free of the effects of surface contamination and surface roughness, so that the resulting optical response functions are thought to be representative of bulk aluminum.

In a second paper,<sup>2</sup> Szmulowicz and Segall reported theoretical values for the interband contribution to the optical conductivity of aluminum. Their calculations utilized the APW band-structure method and included evaluation of transition matrix elements. These authors

found that the interband component of the conductivity is dominated by two strong "parallel-band"<sup>8,9</sup> absorptions at  $\sim 0.6$  and  $\sim 1.6$  eV. In addition, a less intense interband absorption extending to zero energy was predicted.

The parallel-band absorptions, which can be most simply understood in terms of the nearly-free electron model, consist<sup>9,10</sup> of relatively abrupt absorption edges at  $\sim 2|V_K|$  followed by high-energy tails which go over

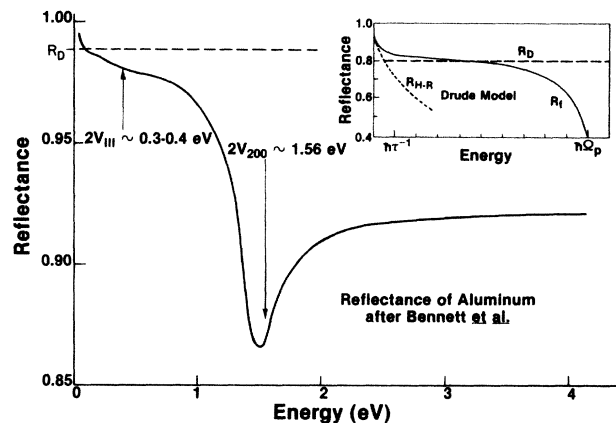


FIG. 1. The reflectance of metallic aluminum films evaporated in ultrahigh vacuum as reported by Bennett *et al.*, Ref. 6. Approximate values of the band gaps at principal Brillouin-zone boundaries are given to indicate the source of the reflectance dips. The inset shows the reflectance ( $R_f$ ) of a metal in the free-electron Drude model for  $\tau^{-1} = 0.1\Omega_p$  and  $\epsilon^b(\omega) = 0.0$ . Given for comparison are the Hagen-Rubens ( $R_{HR}$ ) and Dingle ( $R_D$ ) approximations to the reflectance; for details, see Ref. 39.

into the Butcher interband absorption.<sup>11</sup> Here  $V_{\mathbf{K}}$  denotes the Fourier coefficient of the lattice pseudopotential for reciprocal-lattice vector  $\mathbf{K}$ . The weak low-energy absorption arises<sup>2,12</sup> from a line of "accidental" degeneracies in reciprocal space.

The principal objective of the present study is to compare the calculated interband conductivity of Szmulowicz and Segall with experimental results. This, however, requires a separation of the measured spectrum into intraband and interband components. One might expect such a separation to be a relatively simple matter since intraband effects dominate the dielectric function at sufficiently low energies; by fitting a model of the intraband absorption—for example, the Drude model—to this low-energy region, its contribution to the remainder of the spectrum may be estimated and, in principle, the two components separated. However, the theoretical indication<sup>2</sup> of non-negligible interband contributions below several tenths of an electron volt combined with uncertainties in the experimental values make such an approach—involving large extrapolations—unreliable. The moderately large spread between previously determined Drude parameters—particularly the relaxation time  $\tau$ —might be noted in this connection (e.g., see Table I). Thus, the development of a relatively assumption-free separation procedure, which would utilize experimental data over the full energy range in which the intraband component is large, became a significant aspect of the present analysis.

## II. INTRABAND ABSORPTION

Bennett *et al.*<sup>6</sup> have shown that the free-electron Drude model for the dielectric function,

$$\epsilon^f(\omega) = 1 = \Omega_p^2 / \omega(\omega + i/\tau), \quad (1)$$

gives a good account of the reflectance of aluminum at very low energies ( $<0.1$  eV), where intraband processes are dominant. Here  $\Omega_p$  is the plasma frequency for intraband transitions and  $\tau$  is the intraband relaxation time, which is often expressed in terms of the intraband damping constant  $\gamma = \tau^{-1}$ . More generally, the total linear dielectric function  $\epsilon(\omega) = \epsilon^f(\omega) + \epsilon^b(\omega)$  is the sum of this intraband or "free-carrier" term, and an interband contribution  $\epsilon^b(\omega)$  arising from band-to-band transitions of conduction and core electrons—the classical "bound-electron" absorptions.

Modifications to Drude theory for the anomalous skin effect<sup>13</sup> in good conductors at room temperature lead to essentially the same reflectance as the simple theory, so that the simple model is adequate for present purposes.<sup>14</sup> Moreover, the possibility of frequency-dependent Drude parameters will be dismissed. This is justified both to maintain simplicity and also because theory predicts<sup>15</sup> the absence of such dependence for  $\omega > \omega_{\text{Debye}}$ , which applies here. Early reports of such dependence appear to have arisen before it was appreciated that there were interband absorptions in the energy interval over which the Drude model was being fit.

In aluminum, the Drude parameters cannot be determined with acceptable accuracy by simply fitting the observed reflectivity over the wavelength region dominated

by intraband absorption. The available interval,<sup>6</sup>  $\sim 0.04$  to  $\sim 0.2$  eV, is very short and even a small experimental error in the reflectivity of a good conductor translates into an enormous uncertainty in the refractive index,  $n(\omega) + ik(\omega)$ , when the reflectance is nearly unity as it is for aluminum. For instance, in the present study, fits to the measured reflectance of aluminum below 0.2 eV within the quoted experimental error ( $\pm 0.1\%$ ) were obtained with sets of Drude parameters ranging from  $\hbar\Omega_p = 50$  eV,  $\hbar\gamma = 0.475$  eV to  $\hbar\Omega_p = 10$  eV,  $\hbar\gamma = 0.065$  eV.

This uncertainty may be reduced by employing independently measured quantities relating the Drude parameters and/or by using a qualitative knowledge of the interband spectrum to aid in fitting the Drude model over a wide frequency range. The traditional choice for an independent quantity is the dc conductivity, which in the Drude model is<sup>16</sup>

$$\sigma(0) = \Omega_p^2 / 4\pi\gamma. \quad (2)$$

The intraband plasma frequency  $\Omega_p$  is often expressed in terms of the "effective" number of conduction electrons  $\mathcal{N}_{\text{eff}}$  or, alternatively, the optical mass<sup>17</sup>  $m_{\text{opt}}$  using the definitions

$$\Omega_p^2 = \frac{4\pi\mathcal{N}_{\text{eff}}e^2}{m} = \frac{4\pi\mathcal{N}e^2}{m_{\text{opt}}}. \quad (3)$$

It should be stressed at this point that  $\Omega_p$  in Eqs. (1)–(3) is *not* the observed plasmon frequency nor are  $\mathcal{N}_{\text{eff}}$  and  $m_{\text{opt}}$  of Eq. (3) the actual conduction-electron density  $\mathcal{N}$  or the bare-electron-mass  $m$ . Rather, they are parameters which measure the strength of the intraband part of the conduction-electron spectrum. Specifically,  $\Omega_p$  should not be confused with the frequency of the bulk plasmon  $\omega_p$ , which occurs at the zero of  $\text{Re}\epsilon(\omega)$ . The plasmon involves both intraband and interband processes, the latter through the presence of  $\epsilon^b(\omega)$  in Eq. (1). This point is illustrated in Fig. 2, which displays the real and imaginary parts of a schematic dielectric function for a good conductor with a single strong absorption peak.

In the case of aluminum, this has been a source of considerable confusion in the literature,<sup>18</sup> especially because between approximately 2 to 5 eV the optical properties of aluminum fortuitously fit<sup>19,20</sup> a Drude model, even though the dielectric response in this region is a combination of intraband and interband processes. The Drude model plasma energy for this fortuitous fit is  $\sim 15$  eV, which corresponds to an electron density of roughly three electrons per atom ( $e/\text{atom}$ ), the actual conduction-electron density. It is erroneous to interpret this as implying these are three "free" electrons per atom. Rather, it should be interpreted as showing that the conduction-electron oscillator strength is largely exhausted above 2 or 3 eV. The point is that above this energy, both the intraband and interband contributions to  $\epsilon_1(\omega)$ , the real part of  $\epsilon(\omega)$ , have the same asymptotic behavior as a free-electron gas, and their combination exhibits a plasma frequency corresponding to the total conduction oscillator strength of  $\sim 3.11$   $e/\text{atom}$ . We note in passing that this total conduction-electron oscillator strength exceeds the conduction-electron density (3  $e/\text{atom}$ ) because of the redistribution of core oscillator strength resulting from

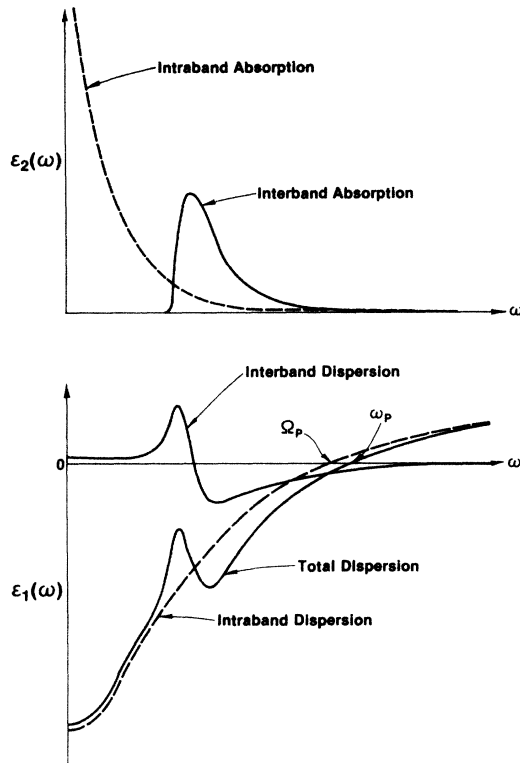


FIG. 2. A schematic representation of the superposition of intraband and interband processes in the complex dielectric function  $\epsilon_1(\omega) + i\epsilon_2(\omega)$ . This indicates the criterion used to separate the two processes, viz., that the Drude contribution to the real part of the dielectric function must pass through the regions of anomalous interband dispersion in the observed total dielectric function. For details, see the text. Also illustrated is the difference between the intraband plasma frequency  $\Omega_p$  and the bulk plasma frequency  $\omega_p$ .

exchange effects.<sup>21-23</sup>

Table I gives some of the more recent literature values for the Drude parameters of aluminum together with the experimental bulk dc conductivity at room temperature. The early work of Mendlowitz<sup>19</sup> involved a Drude fit to optical data above roughly 2 eV so that effects of both the 0.5 and the 1.5 eV interband transitions were inadvertently included in the Drude parameters. This led to a large overestimate of both the number of “free” electrons and their damping factor. As a consequence, the dc conductivity  $\sigma(0)$  was underestimated. [Note that the inclusion of low-energy interband transitions yields an apparent width  $\gamma$ , much greater than the actual intraband width and, hence, by Eq. (2) too small a value of  $\sigma(0)$ .] Similarly, the low-energy interband transition near 0.5 eV was not separated from the intraband term by Ehrenreich *et al.*<sup>8</sup> or by Powell.<sup>24</sup> Hence, their “intraband component” includes a small amount of interband oscillator strength leading to a dc conductivity which is also too low. Dresselhaus *et al.*<sup>25</sup> took account of the interband absorption below 1 eV, but found a shorter intraband lifetime than other workers (aside from Mendlowitz). The

reason for this is not clear from the description of their work.

Bennett *et al.*<sup>6</sup> sought to reduce the uncertainty in their fit by using the measured bulk values of  $\sigma(0)$  and an assumed  $\mathcal{N}_{\text{eff}} = 2.6$  e/atom, a value<sup>26</sup> appropriate for wavelengths in the vacuum ultraviolet. The circumstance arises that they obtained an excellent reproduction of the reflectivity below 0.15 eV, despite using a value of  $\mathcal{N}_{\text{eff}}$  which includes interband processes; this is because the reflectance in the narrow energy range they considered is determined primarily by  $\sigma(0)$ , not  $\mathcal{N}_{\text{eff}}$ —a fact that Bennett and co-workers appreciated.

An alternative approach to determining the Drude parameters is to combine the Drude expression with a simply parametrized model for the interband spectrum and perform a multivariable least-squares fit to the experimental dielectric function. This has been employed by Mathewson and Myers,<sup>27</sup> and by Benbow and Lynch.<sup>28</sup> It was also investigated in the course of the present study. In all these cases the elegant analytic expressions for the interband conductivity due to Ashcroft and Sturm<sup>10</sup> were employed. These expressions are based on a nearly-free-electron two-band model, which neglects interactions with other bands. Recently these interactions have been shown to broaden the Ashcroft-Sturm results and introduce fine structure.<sup>29</sup> Moreover, the Mathewson and Myers<sup>27</sup> study involved fitting ellipsometric data over the range 0.7 to 2.5 eV for which  $(\omega\tau)^2 \gg 1$ , so that in reality their fits only determined the product  $m_{\text{opt}}\tau$ . These two quantities were separated by using an approximate sum-rule argument due to Ashcroft and Sturm.<sup>30</sup>

Although good fits could be obtained using the Ashcroft-Sturm analytic expressions for the interband spectrum (with phenomenological broadening), our experience was that least-square fittings were rather insensitive to electron lifetimes and hence it was felt that the resulting Drude parameters were not reliable; for details see Ref. 31. Moreover, the procedure biases the decomposition in favor of the two-band model for interband processes. A significant point in this connection is that this approximation does not account for the interband transitions from 0 to  $\sim 0.5$  eV so that these are included in the Drude term when the two-band model is employed in fitting. Since our goal was to find the experimental interband spectrum as independently as possible of assumptions about its form, an alternative means of decomposition was sought.

### III. SEPARATION

The uncertainty and bias in determining the Drude parameters can be reduced significantly by using qualitative, but not quantitative, knowledge of the form of the interband component. Specifically, one expects that the total dielectric function should be the sum of intraband and interband terms with the absorptions and the associated dispersions for the principal interband transitions superimposed on the monotonic Drude background. The situation is indicated schematically in Fig. 2 for the real and imaginary parts of the dielectric function in a region including a strong interband absorption.

TABLE I. Drude parameters for the intraband absorption of metallic aluminum at room temperature and 4.2 K. The effective density of electrons  $n_{\text{eff}}$  is given in electrons per atom ( $e/\text{atom}$ ); in aluminum the actual density of conduction electron is 3  $e/\text{atom}$ .

Source	Temp. (K)	$\hbar\Omega_p$ (eV)	Strength		$m_{\text{opt}}$ ( $m_e$ )	$\tau$ ( $10^{-14}$ sec)	Damping		dc conductivity <sup>a</sup>	
			$n_{\text{eff}}$ ( $e/\text{atom}$ )	$\hbar\gamma$ (meV)			Optical	Electrical		
Mendlowitz, Ref. 19	RT	14.1	2.40	1.25	0.12	549	0.44			
Bennett <i>et al.</i> , <sup>b</sup> Ref. 6	RT	14.7	2.60 (input)	1.15	0.801	82.2	3.18 (input)			
Ehrenreich <i>et al.</i> , Ref. 8	RT	12.7	1.94	1.55	0.512	129	1.52		3.18–3.39 <sup>c,d</sup>	
Powell, Ref. 24	RT	12.2	1.80	1.67	0.66	100	1.81			
Dresselhaus <i>et al.</i> , Ref. 25	RT	12.9±0.7	2.0±0.2	1.5±0.15	0.5±0.2	160±60	1.60±0.8			
Mathewson and Meyers, <sup>e</sup> Ref. 27	RT	13.0	2.03	1.48	1.02	64.5	3.14		3.21 <sup>f</sup>	
Benbow and Lynch, <sup>g</sup> (Ref. 28)	4.2	12.7	1.94	1.55 (input)	1.10	60	3.25			
Present study, unconstrained by $\sigma(0)$	RT	12.5±0.3	1.88±0.09	1.60±0.08	1.06±0.12	63±7	3.00±0.3			
Present study, unconstrained by $\sigma(0)$	RT	12.5±0.3	1.88±0.09	1.60±0.08	1.13±0.05	58.5±3.0	3.23 (input)		3.18–3.39 <sup>c,d</sup>	

<sup>a</sup>The optical conductivity at  $\omega=0$  has been calculated from Drude theory using Eq. (2); the electrical values of  $\sigma(0)$  are for dc measurements on bulk samples.

<sup>b</sup>The measured bulk value of  $\sigma(0)$  was assumed and used to fix the ratio  $\Omega_p^2/\gamma$  via Eq. (2). The value of  $n_{\text{eff}}$  was taken from an analysis of La Villa and Mendlowitz, Ref. 26, appropriate to the uv and includes a large interband contribution.

<sup>c</sup>Reference 34.

<sup>d</sup>Reference 35.

<sup>e</sup>Fitting of the combined Drude and Ashcroft-Sturm models yielded the product  $m_{\text{opt}}\tau$ . The factors in the product were then determined by an approximate sum rule argument, Eq. (42) of Ashcroft and Sturm, Ref. 10; see also Ref. 30.

<sup>f</sup>Reference 27.

<sup>g</sup>The value of  $m_{\text{opt}}$  was taken from the results of a fit by Ashcroft and Sturm, Ref. 10.

This line of reasoning suggests that the intraband portion of the observed  $\epsilon(\omega)$  may be determined by choosing the Drude parameters such that when the observed  $\epsilon_1(\omega)$  and the intraband contribution to  $\epsilon_1(\omega)$  are plotted together, the two curves cross at or near the onset of the two principal interband transitions. These crossings correspond to the regions of anomalous dispersion associated with the two strong interband absorptions that are independently predicted from Fermi-surface measurements and the nearly-free electron model to lie near  $\sim 0.5$  and  $\sim 1.6$  eV (Ref. 32) (these values are appropriate for temperatures below 4 K, and small red shifts are expected at room temperature).

To carry out this procedure, a computer graphics display was set up to continuously exhibit both the experimental  $\epsilon(\omega)$  curve and the trial intraband  $\epsilon(\omega)$  while the Drude parameters were varied manually. A representative display for the real part  $\epsilon_1(\omega)$  is shown in Fig. 3 for values of  $\Omega_p$  and  $\gamma$  which give an acceptable fit to the data. As indicated in the figure, the position of the crossings, which are relatively unambiguous, are consistent with the band gaps inferred from Fermi-surface fitting. Our experience was that this procedure settled on Drude parameters within a narrow range of uncertainty relatively quickly.

In the event that the anomalous dispersions are less pronounced than in aluminum, a direct fitting of  $\epsilon_1(\omega)$  may be difficult to implement. The fitting in such cases, however, can generally be facilitated by studying derivative spectra.

The fitting procedure can be made easier and the uncertainty reduced if the additional constraint that the Drude parameters be consistent with  $\sigma(0)$  for the material under study via Eq. (2) is introduced. The use of this auxiliary requirement has been a source of concern in the analysis of optical data for some time, since reflectance measurements are often made on evaporated films, and under certain preparation conditions such films do not exhibit the

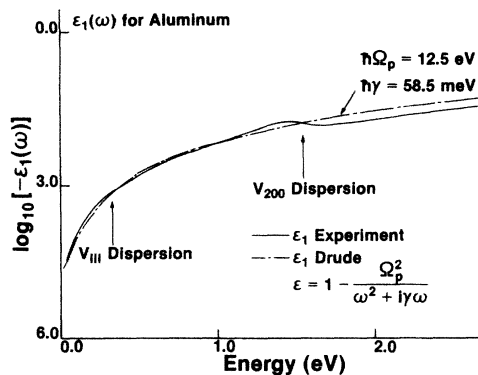


FIG. 3. The real part of the dielectric function of metallic aluminum  $\epsilon_1(\omega)$  at room temperature as determined by Shiles *et al.* (—), with its Drude component (---). The latter was determined by the anomalous dispersion criterion that the two curves cross near the zone-boundary gaps and that the intraband processes dominate at low frequencies. Note that the vertical scale is logarithmic so that although the two curves are approximately parallel above 2.0 eV, the  $\epsilon_1(\omega)$  values actually approach one another as energy increases.

bulk conductivity.<sup>33</sup> However, this objection may be avoided when necessary by simply calculating the appropriate  $\sigma(0)$  for the film under study from the experimental values of  $\epsilon_1(\omega)$  by the “internal” sum rule<sup>3,4</sup>

$$\int_0^\infty [\epsilon_1(\omega) - 1] d\omega = -2\pi^2 \sigma(0). \quad (4)$$

Shiles *et al.*<sup>1</sup> report  $\sigma(0) \approx 3.21 \times 10^{17} \text{ sec}^{-1}$  ( $2.80 \mu\Omega \text{ cm}$ ) from their analysis of the UHV films, which is within the range of conductivity reported for bulk aluminum at room temperature.<sup>34,35</sup>

These separation techniques were applied to the  $\epsilon(\omega)$  results of Shiles *et al.*, both with and without the use of  $\sigma(0)$  as a constraint. The strength of the Drude term was found to be the same in both instances,

$$\hbar\Omega_p = 12.5 \pm 0.3 \text{ eV},$$

while the lifetimes and conductivities differed by only a small amount: unconstrained

$$\tau = (1.06 \pm 0.12) \times 10^{-14} \text{ sec},$$

$$\sigma(0) = (3.00 \pm 0.3) \times 10^{17} \text{ sec}^{-1};$$

constrained by  $\sigma(0)$  as input

$$\tau = (1.13 \pm 0.05) \times 10^{-14} \text{ sec},$$

$$\sigma(0) = 3.23 \times 10^{17} \text{ sec}^{-1}.$$

The limits of error given for these results indicate the

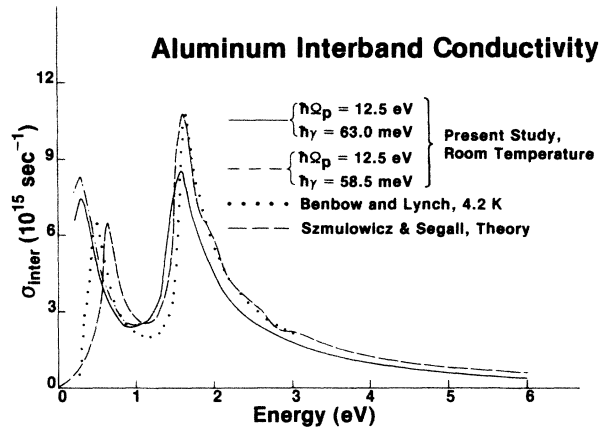


FIG. 4. The interband optical conductivity for metallic aluminum. The results of the present study are given by the solid and the dot-dash curves, which merge for energies above  $\sim 1.1$  eV. These interband conductivities have been derived from the observed optical properties for room-temperature films assuming a Drude interband contribution as described in the text. The solid curve corresponds to the unconstrained result for Drude parameters  $\hbar\Omega_p = 12.5$  eV,  $\hbar\gamma = 63.0$  meV; while the dot-dash curve gives the constrained result with  $\hbar\Omega_p = 12.5$  eV,  $\hbar\gamma = 58.5$  meV. The dotted curve gives the interband component at 4.2 K as determined by Benbow and Lynch, Ref. 28, and the dashed curve is the (broadened) theoretical interband component calculated by Szmulowicz and Segall, Ref. 2, from their parametrized APW band structures as fit to 4.2 K measurements.

range of parameters over which acceptable fits could be obtained.

The constrained result for  $\tau$  is well within the limits of error of the unconstrained values and in both cases the static conductivity  $\sigma(0)$  is consistent with the sum rule value<sup>1</sup>  $3.2_1 \times 10^{17} \text{ sec}^{-1}$  given by Eq. (4) and the experimental values reported for transport measurements on bulk aluminum,<sup>34,35</sup> 3.18 to  $3.39 \times 10^{17} \text{ sec}^{-1}$ .

The experimental interband spectrum is most conveniently expressed in terms of the interband conductivity

$$\sigma^b(\omega) = (-i\omega/4\pi)\epsilon^b(\omega). \quad (5)$$

This may be found directly by subtracting the Drude intraband dielectric function from the total experimental optical dielectric function. The results for both the unconstrained and constrained cases are very nearly the same, differing only slightly (less than 15%) near the peak of the low-energy transition. The results for the real (or absorptive) part of the interband conductivity,  $\sigma_1^b(\omega)$ , for both cases are given in Fig. 4 as examples.

#### IV. DISCUSSION

The experimental interband conductivity shows the two-peak structure expected for parallel-band absorptions near the (100) and (111) Brillouin-zone boundaries in the extended zone of an fcc metal.<sup>10</sup> The high-energy transition at  $\sim 1.5 \text{ eV}$  clearly echos the pronounced drop in the reflectance of aluminum near  $0.8 \mu\text{m}$  (Refs. 1 and 6) evident in Fig. 1. The low-energy transition at  $\sim 0.4 \text{ eV}$  is remarkable in that it has no prominent counterpart in the reflectance spectrum, yet it emerges as a major feature in the interband optical conductivity. An examination of the reflectance data shows, however, that there is a slight but abrupt change in slope between 0.2 and 0.4 eV. Despite the small size of this low-energy change in slope and the fact that it is near the end of the ranges over which the interband conductivity can be meaningfully determined, the corresponding peak in  $\sigma^b(\omega)$  is not an artifact of a particular choice of  $\Omega_p$  and  $\tau$ . The low-energy peak in  $\sigma^b(\omega)$  appears throughout the range of uncertainty of the Drude parameters, and even for a wide range of parameters that would be unacceptable for an overall fit to  $\epsilon(\omega)$ .

The principal uncertainty in  $\sigma^b(\omega)$  arises from uncertainties in the Drude parameters. The high-energy inter-

band transition shows negligible variation in position, width, or height for separations using the extreme values of the permissible range of parameters. The low-energy transition, on the other hand, has a peak-height uncertainty of  $\sim \pm 15\%$  and a width and peak position uncertainty of  $\sim 0.1 \text{ eV}$ . Below about 0.2 eV, uncertainties in  $\sigma^b(\omega)$  are overwhelming.

The experimental interband spectrum derived by Benbow and Lynch<sup>28</sup> for aluminum at 4.2 K is given for comparison with the present room-temperature results in Fig. 4. It is clear that the interband transitions broaden and shift toward lower energies as the temperature rises. A similar trend has been reported by Mathewson and Myers<sup>27</sup> for the 1.5 eV peak at higher temperatures. To within the experimental uncertainty, there is only a small change in interband oscillator strength between liquid helium and room temperatures. At higher temperatures, the intraband absorption grows at the expense of the interband transitions which finally disappear on melting.<sup>36</sup> A comparison of the characteristics of the two principal interband transitions is given in Table II.

The theoretical interband conductivity as calculated by Szmulowicz and Segall<sup>2</sup> from their APW band structure is also given in Fig. 4 for comparison. The band structure was parametrized to yield agreement with Fermi-surface calipers, the  $L_{II,III}$  emission spectrum and, most important here, the value of 1.6 eV for the peak position of the high-energy parallel-band absorption as observed by Bos and Lynch<sup>37</sup> for aluminum at 4.2 K.

The calculated curve is noteworthy in that, while its prominent features are the two parallel-band absorptions, the absorptions do not have the abrupt onset at the zone-boundary gaps,  $2|V_{\mathbf{K}}|$ , predicted by the unbroadened two-band model.<sup>9,10</sup> Rather, they are broadened and the lower-energy transition extends to  $\omega=0$ . These deviations from the two-band model arise from the interaction of three or more bands, particularly near the intersections of Brillouin-zone boundaries. Similar broadening has also been found in recent first-principles calculations of the interband spectrum by Callaway and Laurent.<sup>38</sup>

The broadening is significant and on the low-energy side of the principal transitions it introduces a width at half maximum of  $\geq 50 \text{ meV}$ . This is important for interpreting the phenomenological interband relaxation time  $\tau_i$ , introduced by Ashcroft and Sturm<sup>10</sup> to broaden their

TABLE II. Characteristics of the principal interband transitions in the optical conductivity spectrum of metallic aluminum.

	Low-energy transition		High-energy transition	
	Present study <sup>a</sup> (Room temperature)	Benbow and Lynch (4.2 K)	Present study <sup>a</sup> (Room temperature)	Benbow and Lynch (4.2 K)
Peak position (eV)	0.3–0.4	0.49	1.58	1.64
Height $\sigma_{\text{max}}$ ( $10^{14} \text{ sec}^{-1}$ )	$\sim 70$	65	85	116
Width $\Gamma$ (eV)	$\sim 0.3^b$	0.25 <sup>b</sup>	0.66 <sup>c</sup>	0.5 <sup>c</sup>
Strength in arbitrary units $\sigma_{\text{max}} \times \Gamma$ ( $10^{14} \text{ eV sec}^{-1}$ )	21	16	56	58

<sup>a</sup>Based primarily on the room-temperature reflectance measurements of Bennett *et al.*, Ref. 6.

<sup>b</sup>Right half width at half maximum.

<sup>c</sup>Full width at half maximum.

TABLE III. The oscillator strength per atom  $f$  for the conduction-electron absorption of metallic aluminum. The total oscillator strength exceeds the number of conduction electrons per atom (3) because of the Pauli-principle redistribution of oscillator strength, see Refs. 21–23.

Transition	0 to 7 eV		0 to the $L_{II,III}$ edge present analysis
	Present analysis	Theory Szmulowicz and Segall <sup>a</sup>	
$f_{\text{intraband}}$	$1.87 \pm 0.09^c$		$1.88 \pm 0.09^c$
$f_{\text{interband}}$	$0.91 \mp 0.09^c$	0.97	$1.23 \mp 0.09^c$
$f_{\text{total}}$	2.78		$3.11^b$

<sup>a</sup>Szmulowicz and Segall, Ref. 2.

<sup>b</sup>From the analysis given by Shiles *et al.*, Ref. 1.

<sup>c</sup>The limits quoted refer to the uncertainty in the separation of intraband and interband effects.

two-band model absorptions. In the case of aluminum, a value of  $\tau_i \sim 0.5 \times 10^{-14}$  sec (corresponding to an interband damping  $\gamma_i = 132$  meV) is required<sup>10</sup> to fit the two-band model to the measured spectra. Comparison of this with the 50 meV “band-structure broadening” found by Szmulowicz and Segall shows that a significant contributor to  $\tau_i$  is scattering out of the two-band model states as a result of interactions with other energy bands. This is not a dynamic relaxation involving phonons, rather it is a purely one-electron effect that arises naturally in a full band-structure calculation. Moreover, these considerations imply that the intraband relaxation time for the Drude term  $\tau$ —found here to be  $\sim 1 \times 10^{-14}$  sec ( $\gamma \sim 60$  meV)—and the phenomenological interband relaxation time introduced in the two-band model  $\tau_i$  are not directly comparable since, among the other effects, the latter includes the band-structure broadening.

There is, of course, additional broadening of the interband spectrum as a result of thermal and lattice disorder as well as surface scattering. Szmulowicz and Segall<sup>2</sup> found that the 4.2 K spectrum—for which their crystal potential was parametrized—could be reproduced very closely by including an additional Lorentzian broadening with a weak energy dependence. The full width at half maximum for this additional broadening was  $\sim 0.05$  eV at the low-energy peak and  $\sim 0.07$  eV at the high-energy peak, values which are comparable to the “band-structure” contribution to  $\tau_i$ .

A final point to be noted is the success of the

Szmulowicz-Segall semiempirical calculation in predicting the interband oscillator strength from 0 to 7 eV as 0.94  $e/\text{atom}$  which is in excellent agreement with the “experimental” value found by integrating  $\sigma^b(\omega)$ , viz.,  $0.91 \pm 0.09$   $e/\text{atom}$ ; the details are given in Table III.

#### ACKNOWLEDGMENTS

One of the authors (D.Y.S.) would like to express particular thanks to the late Professor Dr. H. Pick for making the facilities of the Physikalisches Institut (Teil 2) der Universität Stuttgart available to him during part of the study. The other author (B.S.) wishes to thank Professor Dr. O. K. Andersen of the Max-Planck-Institut für Festkörperforschung for his hospitality during the initial stages of this work.

The authors are also happy to acknowledge the considerable assistance of Herr K. Jakobi of the Universität Stuttgart, who aided in setting up specialized computer hardware to facilitate the separation methods developed, and of Frank Szmulowicz of the University of Dayton Research Institute for discussions of details of his calculations. Thanks are also due to Professor D. W. Lynch for providing a tabulation of  $\sigma_{\text{inter}}$  for aluminum from the study of Benbow and Lynch. This work was supported by The U.S. Department of Energy (Basic Energy Sciences—Materials Sciences) under Contract No. W-31-109-Eng-38.

\*Present address: Department of Physics, University of Vermont, Burlington, VT 05405.

<sup>1</sup>E. Shiles, T. Sasaki, M. Inokuti, and D. Y. Smith, Phys. Rev. B **22**, 1612 (1980).

<sup>2</sup>F. Szmulowicz and B. Segall, Phys. Rev. B **24**, 892 (1981).

<sup>3</sup>M. Altarelli, D. L. Dexter, H. M. Nussenzweig, and D. Y. Smith, Phys. Rev. B **6**, 4502 (1972).

<sup>4</sup>D. Y. Smith and E. Shiles, Phys. Rev. B **17**, 4689 (1978).

<sup>5</sup>H. Bichsel and E. A. Uehling, Phys. Rev. **119**, 1670 (1960); C. Tschalär and H. Bichsel, Phys. Rev. **175**, 476 (1968).

<sup>6</sup>H. E. Bennett, M. Silver, and E. J. Ashley, J. Opt. Soc. Am. **53**, 1089 (1963).

<sup>7</sup>J. G. Endriz and W. E. Spicer, Phys. Rev. B **4**, 4144 (1971); **4**, 4159 (1971).

<sup>8</sup>H. Ehrenreich, H. R. Philipp, and B. Segall, Phys. Rev. **132**, 1918 (1963).

<sup>9</sup>W. A. Harrison, Phys. Rev. **147**, 467 (1966).

<sup>10</sup>N. W. Ashcroft and K. Sturm, Phys. Rev. B **3**, 1898 (1971).

<sup>11</sup>P. N. Butcher, Proc. Phys. Soc. London **64A**, 765 (1951).

<sup>12</sup>D. Brust, Phys. Rev. B **2**, 818 (1970).

<sup>13</sup>R. B. Dingle, Physica **19**, 311 (1953); **19**, 348 (1953); **19**, 729 (1953).

<sup>14</sup>H. E. Bennett and J. M. Bennett, in *Optical Properties and Electronic Structure of Metals and Alloys*, edited by F. Abeles (North-Holland, Amsterdam, 1966), p. 175.

<sup>15</sup>G. D. Mahan, *Many-Particle Physics* (Plenum, New York, 1981), Sec. 8.1.G.

<sup>16</sup>See, for example, F. Wooten, *Optical Properties of Solids* (Academic, New York, 1972).

<sup>17</sup>M. H. Cohen, Philos. Mag. **3**, 762 (1958).

<sup>18</sup>See, for example, M. D. Borisov, I. I. Demidenko, and V. G. Padalka, Opt. Spektrosk. **11**, 769 (1961) [Opt. Spectrosc.

- (USSR) 11, 416 (1961)].
- <sup>19</sup>See, for example, H. Mendlowitz, Proc. Phys. Soc. London **75**, 664 (1960).
- <sup>20</sup>W. R. Hunter, J. Opt. Soc. Am. **54**, 208 (1964); J. Phys. (Paris) **25**, 154 (1964).
- <sup>21</sup>R. de L. Kronig and A. H. Kramers, Z. Phys. **48**, 174 (1928).
- <sup>22</sup>V. Fock, Z. Phys. **89**, 744 (1934).
- <sup>23</sup>D. Y. Smith and E. Shiles, in *Recent Developments in Condensed Matter Physics*, edited by J. T. Devreese, L. F. Lemmens, V. E. Van Doren, and J. Van Royen (Plenum, New York, 1981), Vol. 3, p. 323.
- <sup>24</sup>C. J. Powell, J. Opt. Soc. Am. **60**, 78 (1970).
- <sup>25</sup>G. Dresselhaus, M. S. Dresselhaus, and D. Beaglehole, in *Electronic Density of States*, Natl. Bur. Stand. (U.S.) Spec. Publ. No. 323, edited by L. H. Bennett (U.S. GPO, Washington, D.C., 1971), p. 33.
- <sup>26</sup>R. LaVilla and H. Mendlowitz, Phys. Rev. Lett. **9**, 149 (1962).
- <sup>27</sup>A. G. Mathewson and H. P. Myers, J. Phys. F **2**, 403 (1972).
- <sup>28</sup>R. L. Benbow and D. W. Lynch, Phys. Rev. B **12**, 5615 (1975).
- <sup>29</sup>D. Y. Smith, D. D. Koelling, and B. Segall, Bull. Am. Phys. Soc. **28**, 387 (1983).
- <sup>30</sup>Ashcroft and Sturm, Ref. 10, apply the  $f$  sum rule for the transverse conductivity to the conduction electrons to show that the sum of the intraband oscillator strength  $m/m_{\text{opt}}$  and the interband oscillator strengths  $S_K$  for a conduction electron obey [Ref. 10, Eq. (38)]  $m/m_{\text{opt}} + S_K = 1$ . This formulation neglects a small redistribution of oscillator strength between core and valence electrons arising from the Pauli principle, see Refs. 21–23. This redistribution increases the conduction-electron absorption and to a first approximation may be included in the Ashcroft-Sturm result by replacing unity by the ratio of the net conduction-electron oscillator strength density to the number density of conduction electrons. Shiles *et al.*, Ref. 1, found this ratio to be  $3.11/3 \approx 1.04$ . A recalculation of the Mathewson and Myers Drude parameters for this factor yields  $m_{\text{opt}} = 1.40$  rather than 1.48, and  $\tau = 1.08 \times 10^{-14}$  sec in place of  $1.02 \times 10^{-14}$  sec.
- <sup>31</sup>Least-squares fitting of the Drude and Ashcroft-Sturm formulas to  $\sigma(\omega)$  in principle involves five independent parameters: the Drude parameters  $\Omega_p$  and  $\tau$ , the pseudopotentials  $V_{200}$  and  $V_{111}$ , as well as the phenomenological interband lifetime  $\tau_i$ . In most least-squares fitting studies, the problem has been reduced to a four-parameter minimization by using auxiliary conditions on the Drude term; e.g., assuming  $m_{\text{opt}}$  (Ref. 28), using the bulk dc conductivity (present work), or by exploiting the  $f$  sum rule (Ref. 27, see also Ref. 30). In the least-squares fits made for the present study, the  $\text{Re}\sigma(\omega)$  results of Shiles *et al.* were fit over the range 0.04 to 2.5 eV. Below  $\sim 0.5$  eV, the Drude term is large and dominates the fit over the entire energy range. In the usual least-squares fitting procedure, this leads to a good fit of the Drude term at the expense of fitting the weaker interband term well. As an alternative, a second fitting criterion was used which minimized the relative error as measured by the total of the squares of the errors as normalized by  $\text{Re}\sigma(\omega)$ . The difference between the parameter sets given by the two fitting methods was taken as the uncertainty in the fits. The average results were  $\hbar\Omega_p = 13.0 \pm 0.5$  eV,  $V_{111} = 0.15 \pm 0.01$  eV,  $\tau = (1.1 \pm 0.1) \times 10^{-14}$  sec,  $V_{200} = 0.722 \pm 0.002$  eV,  $[m_{\text{opt}}\tau = (1.6 \pm 0.3) \times 10^{-14}$  sec],  $\tau_i = (0.45 \pm 0.11) \times 10^{-14}$  sec. These results—especially  $V_{111}$ —differ somewhat from the room-temperature results of Mathewson and Myers (Ref. 27) [ $m_{\text{opt}}\tau = 1.51 \times 10^{-14}$  sec,  $V_{111} = 0.190$  eV,  $V_{200} = 0.738$  eV, and  $\tau_i = 0.38 \times 10^{-14}$  sec], which were obtained by fitting ellipsometric measurements covering the range 0.7 to 2.50 eV. Aside from different experimental uncertainties in starting data, a possible explanation may be that Mathewson and Myers's data include the tail, but not the peak of the low-energy interband transition.
- <sup>32</sup>As calculated from the Fourier coefficients of the crystal potential given by N. W. Ashcroft, Philos. Mag. **8**, 2055 (1963). See also J. R. Anderson and S. S. Lane, Phys. Rev. B **2**, 298 (1970).
- <sup>33</sup>See, for example, A. I. Golovashkin, G. P. Motulevich, and A. A. Shubin, Zh. Eksp. Teor. Fiz. **38**, 51 (1960) [Sov. Phys.—JETP **11**, 38 (1960)].
- <sup>34</sup>*Handbook of Chemistry and Physics*, 58th ed., edited by R. C. Weast (CRC, Cleveland, 1977); *Handbook of Chemistry and Physics*, 64th ed., edited by R. C. Weast (CRC, Boca Raton, 1983).
- <sup>35</sup>G. T. Meaden, *Electrical Resistance of Metals* (Plenum, New York, 1965).
- <sup>36</sup>J. C. Miller, Philos. Mag. **20**, 1115 (1969).
- <sup>37</sup>L. W. Bos and D. W. Lynch, Phys. Rev. Lett. **25**, 156 (1970).
- <sup>38</sup>J. Callaway and D. G. Laurent, Phys. Lett. **84A**, 499 (1981). The interband spectrum of aluminum was predicted from a self-consistent band calculation based on the local-density-functional approach with a Kohn-Sham exchange term. The resulting  $\sigma^b(\omega)$  exhibits a strong peak at 1.6 eV in agreement with experiment, but the absorption falls off less rapidly at high energies than the measured values, even without the introduction of lifetime broadening. A second departure from experiment is the weakness of the calculated low-energy peak, as well as its location at 0.85 eV. As evidenced in a number of other studies, the density-functional approach has been less successful in dealing with excited states than with the ground states for which it was designed.
- <sup>39</sup>F. A. Modine and D. Y. Smith, J. Opt. Soc. Am. A **1**, 1171 (1984).